J. Fluid Mech. (1974), *vol.* 65, *part* 4, *pp.* 769–779
Printed in Great Britain

The stability of a trailing line vortex. Part 2. Viscous theory

By MARTIN LESSEN AND FREDERICK PAILLET

Department of Mechanical and Aerospace Sciences,
University of Rochester, New York 14627

(Received 29 October 1973 and in revised form 22 March 1974)

In a previous paper, the inviscid stability of a swirling far wake was investigated, and the superposition of a swirling flow on the axisymmetric wake was shown to be initially destabilizing, although all modes investigated eventually become more stable at sufficiently large swirl. The most unstable disturbances were non-axisymmetric modes with negative azimuthal wavenumber n representing helical wave paths opposite in sense to the wake rotation. The disturbance growth rate appeared to increase continuously with $|n|$, while all modes with $|n| > 1$ represented disturbances which are completely stable for the non-swirling wake. In the present analysis, both timewise and spacewise growth rates are calculated for the lowest three negative non-axisymmetric modes ($n = -1$, -2 and -3). Vortex intensity is characterized by a swirl parameter q proportional to the ratio of the maximum swirling velocity to the maximum axial velocity defect. The large wavenumbers associated with the disturbances at large $|n|$ allow the $n = -1$ mode to have the minimum critical Reynolds number of 16 ($q \simeq 0{\cdot}40$). The other two modes investigated have minimum Reynolds numbers on the neutral curve of 31 ($n = -2$, $q = 0{\cdot}60$) and 57 ($n = -3$, $q = 0{\cdot}80$). For each mode, the neutral-stability curve is shown to shift rapidly towards infinite Reynolds numbers once the swirl becomes sufficiently large. Some of the most unstable swirling flows are shown to possess spacewise amplification factors almost ten times that for the most unstable wavenumber for the non-swirling wake at moderate Reynolds numbers.

1. Introduction

Much effort has been expended both experimentally and theoretically in recent attempts to understand the properties of aircraft trailing vortices. In part 1 of the present study (Lessen, Singh & Paillet 1974) we considered the inviscid stability of a wake and vortex system designed to resemble qualitatively the flow in just such a trailing vortex, and found that the far wake flow became stable, for given azimuthal wavenumber n, only when the vortex intensity had reached a fairly large value. The mean flow assumed for the analysis was the Lamb (1932, p. 592) exponential vortex superimposed on the self-similar axisymmetric wake. The problems involved in relating this assumed flow to that in a real aircraft vortex were readily admitted, but such an approximation should

be more realistic than the discontinuous patching of a rigid-body rotating jet and potential vortex used in some previous studies (for instance, see Uberoi, Chow & Narain 1972; Lessen, Deshpande & Hadji-Ohanes 1973).

The analysis in part 1 was originally undertaken to determine how the stable vorticity distribution of a trailing vortex acts to stabilize the normally unstable axial flow in the vortex core. The laminar Reynolds number of aircraft wakes is approximately 10^6 while the Reynolds number based on a turbulent viscosity is still very large, so that use of the inviscid equations seemed appropriate. However, the inviscid results indicated that the flow became even more unstable in the presence of moderate swirl, with growth rates increasing as the magnitude of the disturbance wavenumber n (< 0) increased; that is, the largest growth rates αc_i and associated values of the axial wavenumber α increased continuously with $|n|$. Thus the question of how viscosity, even at high Reynolds numbers, interferes with disturbances of high (negative) wavenumber becomes important. At the same time, the extremely high growth rates (compared with the axisymmetric wake alone) obtained for moderately swirling flow merit further investigation in their own right.

Attempts to apply similarity arguments to the fully turbulent trailing vortex (such as those of Hoffman & Joubert 1963; Saffman 1973) have indicated that turbulent swirling flows cannot be consistently described by a constant eddy viscosity. The constant eddy viscosity model has been adopted, however, as the only direct means of obtaining a solution for the case of disturbances of high (negative) wavenumber. The results will still be rigorously valid in the case of laminar flows, and will provide some insight into the interaction of shear and rotation in more realistic flows (such as might be relevant to chemical mixing problems).

2. Disturbance equations and numerical solution

As in part 1, the vortex intensity is characterized by the swirl parameter q, which is proportional to the ratio of the maximum swirling velocity to the maximum axial velocity defect. The same mean velocity profiles are examined with respect to non-axisymmetric disturbances:

$$\left.\begin{aligned} u = U(r)+u', \quad v = V(r)+v', \quad w = W(r)+w', \\ U = \exp(-r^2), \quad V = 0, \quad W = qr^{-1}[1-\exp(-r^2)], \\ p = P_0+p', \end{aligned}\right\} \tag{1}$$

$$q = \frac{C_0}{2\pi U_s r_s}, \quad C_0 = \lim_{r\to\infty}(2\pi r v), \quad r_s\left(\frac{4\nu x}{U_0}\right)^{\frac{1}{2}},$$

where (u, v, w) are the (r, ϕ, x) velocity components, U_s is the maximum wake velocity defect as given by Batchelor (1964) and U_0 is the free-stream velocity. All quantities appearing above have been non-dimensionalized with respect to the length scale r_s and the velocity scale U_s. These profiles are shown in figure 1.

The linearized disturbance equations for u', v' and w' may be derived from the viscous incompressible Navier–Stokes equations in a manner similar to that

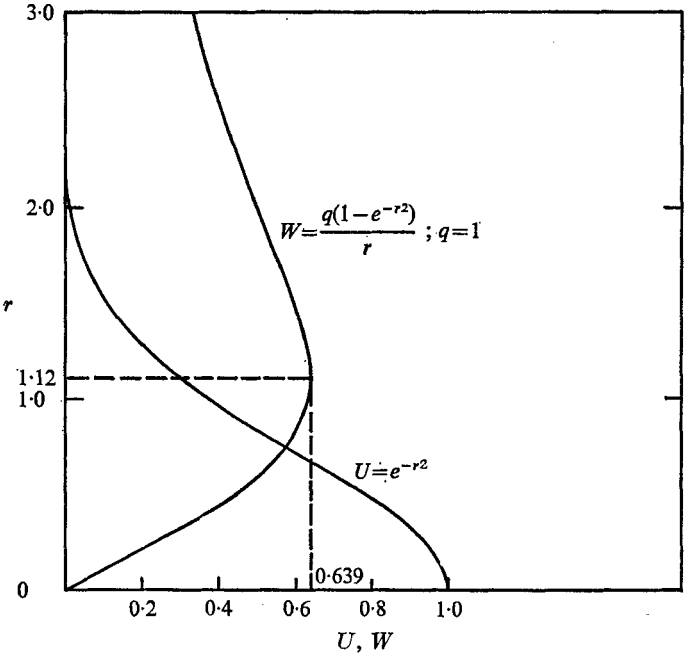

FIGURE 1. The mean velocity profiles $U(r)$ and $W(r)$.

given by Lessen & Singh (1973). Using their notation, perturbation quantities of the following form are assumed:

$$\{u', v', w', p'\} = \{F(r),\ iG(r), H(r), P(r)\} \exp[i(\alpha x + n\phi - \alpha ct)],$$

where either $c = c_r + ic_i$ with α real or $\alpha = \alpha_r + i\alpha_i$ with αc real. Upon substitution into the linearized perturbation equations, the following set of equations results:

$$r^2\gamma F + r^2GU' + \alpha^2 r^2 P = (iR)^{-1}[r(rF')' - (\alpha^2 r^2 + n^2)F], \tag{2a}$$

$$r^2\gamma G + 2rHW - r^2P' = (iR)^{-1}[r(rG')' - (\alpha^2 r^2 + n^2 + 1)G - 2nH], \tag{2b}$$

$$r^2\gamma H + r^2G\overline{W} + rnP = (iR)^{-1}[r(rH')' - (\alpha^2 r^2 + n^2 + 1)H - 2nG], \tag{2c}$$

$$\alpha rF + (rG)' + nH = 0, \tag{2d}$$

where a prime denotes d/dr, $R = r_s U_s/\nu$ and

$$\gamma = \alpha(U - c) + \frac{nW}{r}, \quad \overline{W} = \frac{dW}{dr} + \frac{W}{r}.$$

That equations (2) define a sixth-order system can be seen by using (2*d*) to eliminate G'' from (2*b*), reducing the order of that equation by one.

The boundary conditions associated with these equations are derived from the requirement that all disturbance quantities vanish at large radius, and that all quantities remain bounded and single valued at $r = 0$. These latter conditions are discussed by Batchelor & Gill (1962), and become in the notation used here

$$\left.\begin{aligned} F(0) = G(0) = H(0) = P(0) = 0 \quad &\text{when} \quad n \neq 1, 0, \\ F(0) = G(0) + H(0) = P(0) = 0 \quad &\text{when} \quad n = 1. \end{aligned}\right\} \tag{3}$$

Since no simple solution to these equations can be found, the characteristic disturbance growth rates must be found numerically. To do this most conveniently the equations are transformed into a set of six first-order differential equations:

$$dZ_i/dr = A_{ij}Z_j, \tag{4}$$

where $\{Z_i\} = \{F, G, H, rP, rF', rH'\}$,

$$\{A_{ij}\} = \begin{bmatrix} 0 & 0 & 0 & 0 & r^{-1} & 0 \\ -\alpha & -r^{-1} & -n/r & 0 & 0 & 0 \\ 0 & 0 & 0 & 0 & 0 & r^{-1} \\ 0 & \alpha(U-c)r+nW + \left(\alpha^2+\frac{n^2}{r^2}\right)r\frac{1}{iR} & 2W+\frac{n}{irR} & \frac{1}{r} & \frac{\alpha}{iR} & \frac{n}{irR} \\ \left(\alpha^2+\frac{n^2}{r^2}\right)+iRnW +i\alpha rR(U-c) & iRrU' & 0 & i\alpha R & 0 & 0 \\ 0 & iRr\overline{W}+\frac{2n}{r} & \left(\alpha^2+\frac{n^2+1}{r^2}\right)r+inRU +iRr\alpha(U-c) & \frac{iRn}{r} & 0 & 0 \end{bmatrix}.$$

These six first-order homogeneous ordinary differential equations and the associated boundary conditions define an eigenvalue problem for the various parameters that appear in the equations. A stability investigation normally consists of a systematic search for the complex phase speed (and hence the disturbance growth rate) as a function of the other parameters. If spacewise amplification is sought, the frequency is assumed to be real and the complex wavenumber becomes the eigenvalue.

The use of cylindrical co-ordinates introduces an artificial singularity at the origin which may be treated by standard power-series methods. Equations (4) may be arranged in the form

$$\frac{d}{dr}Z_i = \frac{B_{ij}}{r}Z_j + \sum_{k=0}^{\infty} A_{ij}^{(k)} r^k Z_j, \tag{5}$$

where power-series expansions for $U(r)$ and $W(r)$ have been substituted in (4) before rearrangement to ensure that the matrices $\{A_{ij}^{(k)}\}$ and $\{B_{ij}\}$ contain only constants. This formulation shows that the equations are regularly singular at $r = 0$; and power-series solutions valid near $r = 0$ may be constructed by the method of Frobenius (where the eigenvalues of B_{ij} are the six roots of the indicial equation). After enforcement of the boundary conditions, three vector solutions remain and may be programmed for recursive numerical evaluation. Unfortunately, the series can be summed with useful accuracy only for quite small values of r.

The perturbation equations (2) also possess an irregular singularity at $r = \infty$. Under these circumstances there are techniques for constructing approximate

solutions that are asymptotically valid near the singularity. Equations (2) can be conveniently rearranged in the form

$$dY_i/dr = \hat{A}_{ij} Y_j \tag{6}$$

under the approximation that $U(r) \simeq 0$ and $W(r) \simeq q/r$, which becomes quite accurate for $r > 3$, where

$$\{Y_i\} = \{F, G, H, P, F, H\},$$

$$\{\hat{A}_{ij}\} = \begin{bmatrix} 0 & 0 & 0 & 0 & 1 & 0 \\ -\alpha & -r^{-1} & -n/r & 0 & 0 & 0 \\ 0 & 0 & 0 & 0 & 0 & 1 \\ 0 & -\frac{i}{R}\left[\left(\beta^2+\frac{n^2}{r^2}\right)+\frac{nq}{r^2}\right] & \frac{2q}{r^2}-\frac{in}{r\beta^2} & 0 & -\frac{i\alpha}{R} & -\frac{in}{R} \\ \beta^2+\frac{n^2}{r^2}+\frac{nq}{r^2} & 0 & 0 & i\alpha R & -\frac{1}{r} & 0 \\ 0 & \frac{2n}{r^2} & \beta^2+\frac{n^2+1}{r^2}+\frac{nq}{r^2} & \frac{inR}{r} & 0 & -\frac{1}{r} \end{bmatrix},$$

with $\beta^2 \equiv \alpha^2 - i\alpha Rc$. According to the methods given in Wasow (1965, p. 111), a uniformly valid asymptotic approximation to the solution at large radii may be obtained in the form

$$\mathbf{Y} \simeq \exp(\mathbf{Q}(r))\, r^{\mathbf{D}}\, \mathbf{Z}(r), \quad \text{where} \quad Z_i \simeq \sum_{k=0}^{\infty} b_k^{(i)} \frac{1}{r^k}, \quad \text{as} \quad r \to \infty \quad \text{for} \quad r \in S.$$

$\mathbf{Q}$ is a diagonal matrix in which each element is a polynomial in r, and $\mathbf{D}$ is a constant diagonal matrix. The solution will be valid only in some open sector S of the complex r plane about the singularity. The theory, using the form (6) of the differential equations, shows that the order of the highest-order polynomials in $\mathbf{Q}$ is one, and that S is a sector about the positive real r axis with angle less than π.

Rather than using the involved procedure outlined by Wasow, the asymptotic solutions can be obtained by assuming a solution of the form

$$Y_i = e^{\lambda r} r^D \sum_{k=0}^{\infty} b_k^{(i)} \frac{1}{r^k},$$

substituting this in the equations and comparing like powers of r^{-1}. Eigenvalue problems arise which determine whether such a solution can exist at all, thus determining what values λ and D must take. This procedure gives $\lambda = \pm\alpha$ and $\lambda = \pm\beta$ (twice), with $D = -\frac{1}{2}$ in all cases. The three solutions corresponding to $\lambda = +\alpha$ and $\lambda = +\beta$ (twice) must be discarded to satisfy the boundary conditions, leaving three solutions here also. Then a program to calculate the coefficients in the series $Z_i = \Sigma b_k^{(i)} r^{-k}$ can be written to approximate these remaining three solutions.

The three asymptotic solutions discussed are solutions to the asymptotically valid form of the differential equations. These latter equations have been found to possess one set of solutions which corresponds to the two solutions that remain

when the viscosity is formally set equal to zero. One of these solutions must be discarded according to the boundary conditions; the other is

$$\{F, G, H, P\} = \left\{K_n(\alpha r),\ -K_n'(\alpha r),\ \frac{nK_n(\alpha r)}{\alpha r},\ \left[c - \frac{nq}{\alpha r^2}\right] K_n(\alpha r)\right\},$$

where K_n an nth-order modified Bessel function. This solution may be calculated at any radius directly as long as the approximation $W \simeq q/r$ is valid; the other two solutions must still be calculated using asymptotic series.

Having thus started solutions at each end of the region, the starting solutions are advanced by Taylor series outward from $r = 0$ and inward from $r = r_\infty$ to match at an intermediate radius. This scheme was used because of the presence of solutions which grow like $e^{\beta r}$ for large radii as r increases, since β is usually a large number. The inner solutions can be integrated to a large radius where the potential-vortex approximation to the equations is valid, but not much beyond since random numerical errors will grow to overwhelm the starting solutions. The asymptotic series must, however, be calculated at quite large radii to ensure accuracy. Fortunately, the two outer solutions which grow most rapidly as the integration proceeds inwards can be obtained through numerical integration independently of the third, slower-growing solution, which may be calculated analytically at any radius ($r > 3{\cdot}0$).

The eigenvalue (complex phase speed) is found by matching the inward- and outward-integrated solution vectors at some intermediate radius for a particular fixed pair (α, R). The result is a 6×6 complex determinant whose zeros determine the real and imaginary parts of the phase velocity. The value of the determinant was calculated using a method involving Gaussian elimination, and the Newton–Raphson method was used to iterate to the zeros of the matching determinant.

3. Results and discussion

The original intent behind performing the viscous calculations was to trace the shift of minimum Reynolds numbers on the neutral-stability curves for various n as the swirl intensity q was increased. A uniform transition through large but still finite Reynolds numbers appropriate for actual trailing vortices was anticipated, and the computer program was written to deal with large R. The behaviour associated with a fixed point in the α, R plane as q is increased for $n = +1, -1, -2$ and -3 is indicated in figure 2. The stabilization at large q for these modes is typical of that noted for several test points in the α, R plane. To clarify the way in which stabilization occurs, the Reynolds number corresponding to a point on the neutral curve (with α fixed to correspond to the most unstable wavenumber at large q) was followed as q was increased. The results are shown in figure 3. Rather than shifting at a uniform rate, this R on the neutral curve reaches some minimum value for each $n < 0$, and remains very close to this value for a large range of q before rapidly approaching very large values over a fairly short range of swirl. Stabilization occurs at higher values of q for $n = -2$ and -3 than for $n = -1$, but in all three cases the rate of increase of R becomes

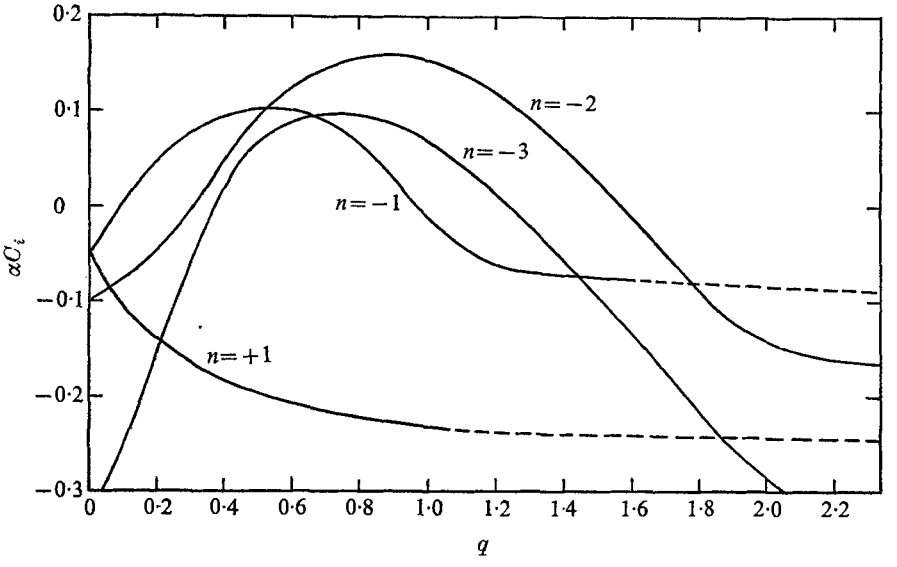

FIGURE 2. Growth rate αC_i *vs.* q at fixed $\alpha = 1{\cdot}34$ and $R = 141{\cdot}4$.

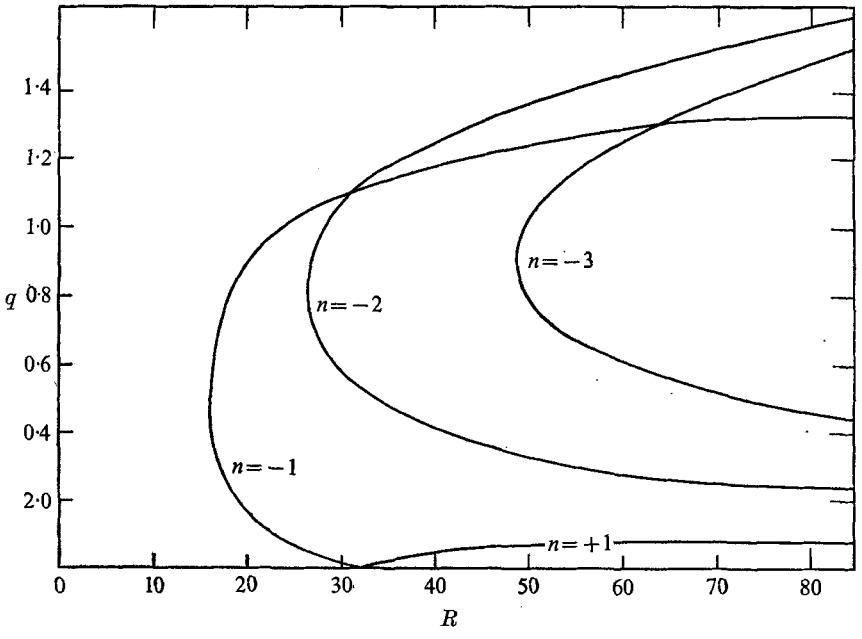

FIGURE 3. Reynolds number corresponding to a point on the neutral-stability curve *vs.* q for various n.

almost infinite for Reynolds numbers less than 300. Investigation of timewise and spacewise growth rates showed that the range of q preceding stabilization was characterized by a regime in which the curves of constant growth became separated by successively greater distances, while the neutral-stability curve hardly shifted at all. Only when the growth rate became very small throughout

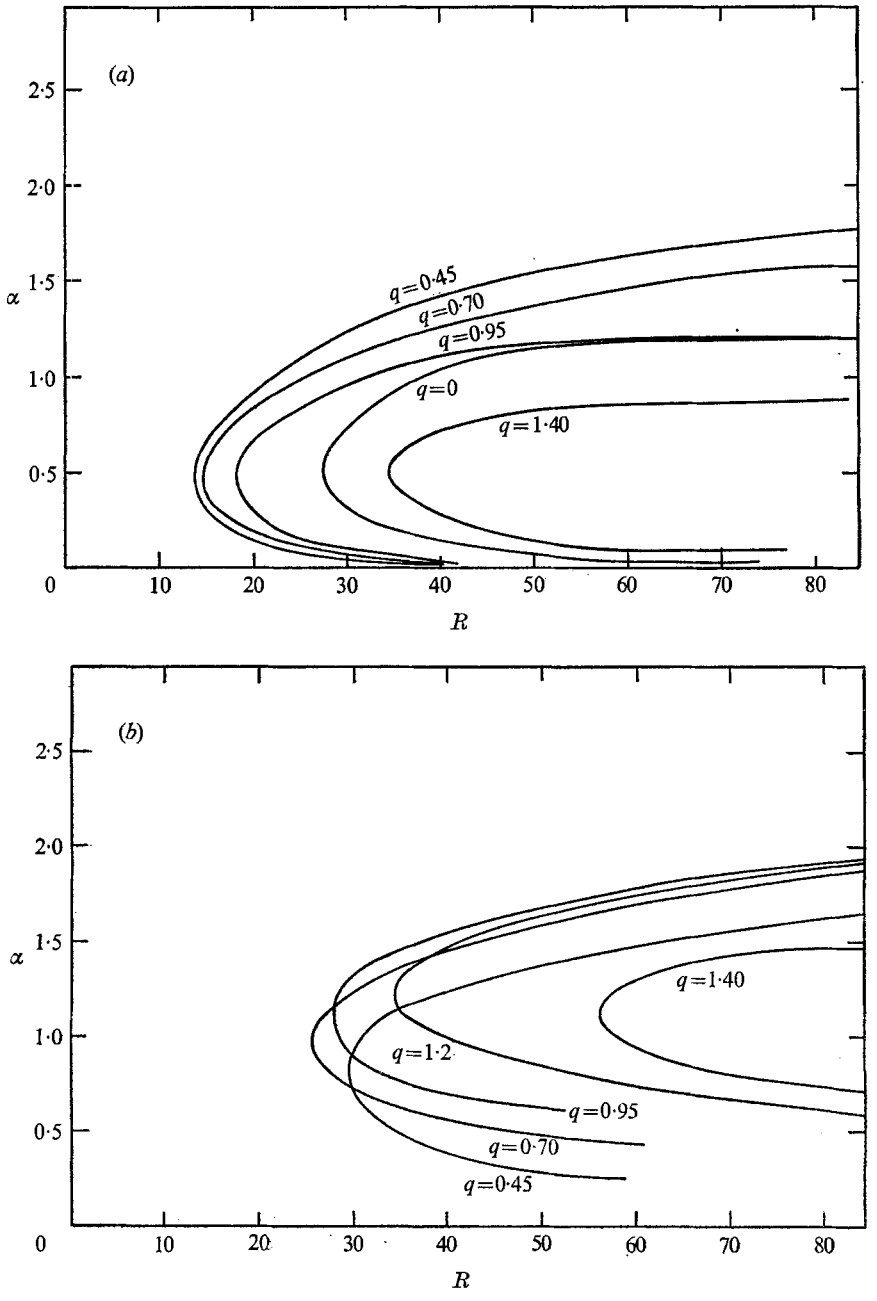

FIGURES 4(*a*), (*b*). For legend see facing page.

the unstable region of the $-R$ half-plane did the neutral curve move rapidly towards large R.

The behaviour illustrated in figure 3 does not rigorously represent the minimum critical Reynolds number $R_c(n)$ for each n, since the critical α shifts with q. For this reason, and to estimate the absolute minimum critical R, neutral-stability

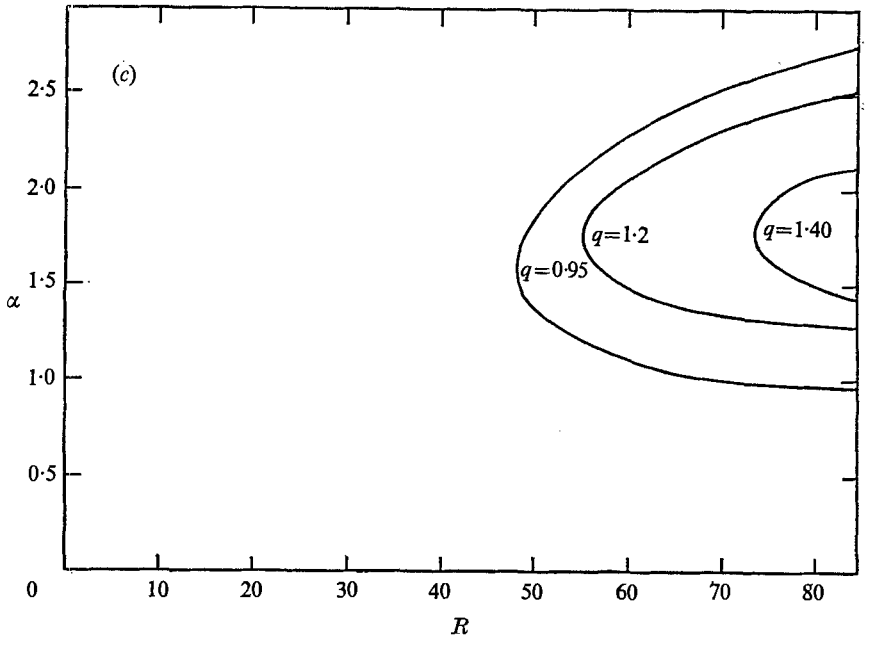

FIGURE 4. Neutral-stability curves in the α, R plane for (*a*) $n = -1$, (*b*) $n = -2$, and (*c*) $n = -3$ and various q.

curves were constructed for $n = -1$, -2 and -3 for successive values of q; some of these curves are shown in figures 4(*a*)–(*c*). The curves also show that neither α_c nor R_c is very sensitive to the exact value of q, and that the most unstable q and α agree with the inviscid results of part 1. (Although the α_c and q_c associated with R_c differ slightly from the most unstable parameters in part 1, the location of constant-growth curves showed good correspondence as $R \to \infty$.) The neutral-stability curve for $n = -1$ and $q = 0{\cdot}25$ and $0{\cdot}6$, for example, could not be plotted in figure 4(*a*) without becoming confused with the curve for $q = 0{\cdot}45$ (which is plotted) in the parameter region near R_c. In view of the computational expense required to find each eigenvalue and the complicated but very weak variation of $R_c(n, q)$, the R_c and the associated axial wavenumbers $\alpha_c(n, q)$ were determined (to at least two decimal places) from these curves. The results are summarized in table 1, where the R_c for $n = -1$, -2 and -3 are listed along with the associated α and q and where the related cases of most unstable inviscid flow from part 1 are also listed for comparison.

The results show that, at the Reynolds numbers appropriate for an actual aircraft wake, the transition from unstable to stable flow situations is probably a sharp function of swirl intensity, and that at least several modes of higher (negative) azimuthal wavenumber may be important even in the presence of turbulent mixing. The absolute minimum R_c is associated with the lowest (negative) non-axisymmetric mode, but higher modes become dominant at moderate R. A comparison in figure 5 of spacewise growth rates for three highly unstable swirling flow modes and the growth rates for the non-swirling wake (rescaled

Inviscid (case of largest growth rate αc_i)

n	$\alpha_{\max}$	αc_i	$q_{\max}$
−1	0·3	0·1470	0·32
−2	1·2	0·3138	0·70
−3	1·7	0·3544	0·79
−4	2·15	0·3777	0·82
−5	2·6	0·3912	0·83
−6	3·2	0·4008	0·83

Viscous (case of minimum critical Reynolds number)

n	α_c	R_c	q_c
−1	0·42	13·9	0·45
−2	0·91	27·9	0·7
−3	1·62	48·2	0·95

TABLE 1. Most unstable situations calculated for both inviscid and viscous cases.

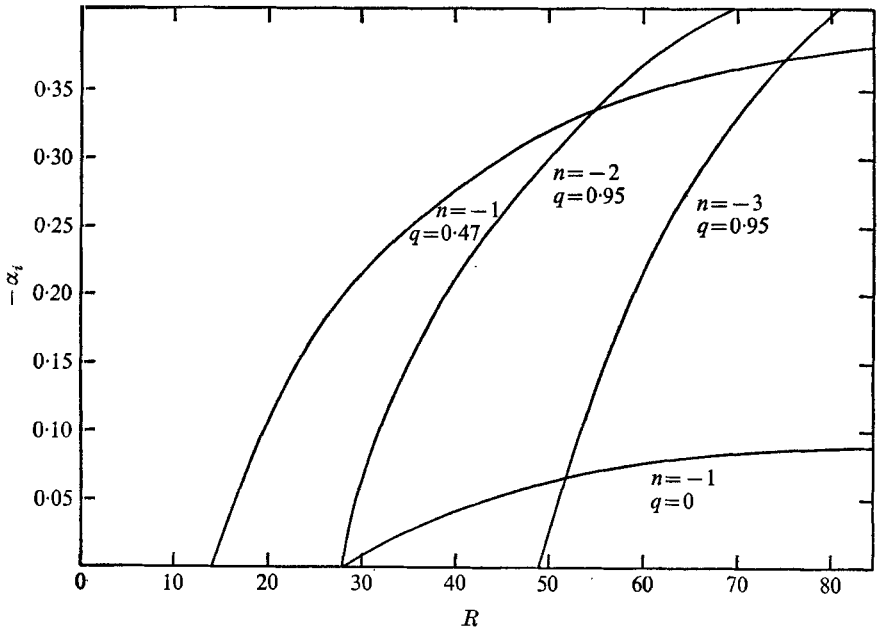

FIGURE 5. Spacewise amplification plotted *vs.* R for three highly unstable cases and for the wake without swirl ($n = 1$, $q = 0$).

from Lessen & Singh 1973) shows how quickly the higher modes dominate as R increases. The viscous analysis of flow in a rotating pipe by Pedley (1969) results in a set of curves remarkably similar to those in figure 3 for the swirling wake. The close similarity with Pedley's (1968) results for the inviscid case were discussed in part 1, but it should be noted that the asymptotic situation he considered corresponds to the case of fixed q, while variation with q is of primary importance here. The profile considered by Bergman (1969) in an inviscid study

of a closely allied flow showed the continued presence of instability at large swirl, but the growth rate became very small and remained confined to extremely small α for larger swirl parameters than those at which the vortex considered here is stabilized. A comparison of the inviscid results for the Lamb exponential vortex with Bergman's eigenvalues was not pursued in great detail in part 1. However, the indication of complete stabilization at finite swirl is supported by the viscous analysis described in this paper. The main difference between the two cases lies in the swirling component of flow since $W = O(r)$ as $r \to 0$ here, while $W = O(r^2)$ for Bergman's model (U and V being essentially the same). It is quite possible that the stability characteristics of the problem are sensitive to this difference, as the critical layer (where $\gamma(r_c) = 0$) occurs at small radius ($r_c \sim 0{\cdot}01$) for the most unstable non-axisymmetric modes. In comparing his results with the behaviour of actual meteorological vortices, Bergman surveyed available data for dust devils and tornadoes and concluded that the typical case corresponded to a q between 2·5 and 5·0 (with a minimum observed case of $q \sim 2{\cdot}0$). These values imply complete stabilization at the swirl intensities for which stabilization of the Lamb vortex is indicated, while the model adopted by Bergman exhibits at least several highly unstable modes at the same swirl. Thus the stability characteristics of these vortices may be of some help in finding the correct velocity distributions for atmospheric vortices.

The authors wish to acknowledge the Control Criteria Branch of the Air Force Flight Dynamics Laboratory (AFFDL/FGC), which provided the computational facilities required for the calculations presented in this paper.

REFERENCES

BATCHELOR, G. K. 1964 Axial flow in trailing line vortices. *J. Fluid Mech.* **20**, 645.

BATCHELOR, G. K. & GILL, A. E. 1962 Analysis of the stability of axisymmetric jets. *J. Fluid Mech.* **14**, 529.

BERGMAN, K. H. 1969 On the dynamic instability of convective atmospheric vortices. Ph.D. thesis, Dept. of Atmospheric Sciences, University of Washington.

HOFFMAN, E. R. & JOUBERT, P. N. 1963 Turbulent line vortices. *J. Fluid Mech.* **16**, 395.

LAMB, H. 1932 *Hydrodynamics*, 6th ed. Dover.

LESSEN, M., DESHPANDE, N. V. & HADJI-OHANES, B. 1973 Stability of a potential vortex with a non-rotating and rigid-body rotating top-hat jet core. *J. Fluid Mech.* **60**, 459.

LESSEN, M. & SINGH, P. J. 1973 The stability of axisymmetric free shear layers. *J. Fluid Mech.* **60**, 433.

LESSEN, M., SINGH, P. J. & PAILLET, F. L. 1974 The stability of a trailing line vortex. Part 1. Inviscid theory. *J. Fluid Mech.* **63**, 753.

PEDLEY, T. J. 1968 On the instability of rapidly rotating shear flows to non-axisymmetric disturbances. *J. Fluid Mech.* **31**, 603.

PEDLEY, T. J. 1969 On the instability of viscous flow in a rapidly rotating pipe. *J. Fluid Mech.* **35**, 97.

SAFFMAN, P. G. 1973 Structure of turbulent line vortices. *Phys. Fluids*, **16**, 1181.

UBEROI, M. S., CHOW, C. Y. & NARAIN, J. P. 1972 Stability of coaxial rotating jet and vortex of different densities. *Phys. Fluids*, **15**, 1718.

WASOW, W. 1965 *Asymptotic Expansions for Ordinary Differential Equations*. Interscience.